Development and calibration of a model for the potential establishment and impact of *Aedes albopictus* in Europe

S. Pasquali[1], L. Mariani[2,3], M. Calvitti[4], R. Moretti[4], L. Ponti[4,5], M. Chiari[6], G. Sperandio[7,8], G. Gilioli[7]

[1] CNR-IMATI "Enrico Magenes", Via A. Corti 12, 20133 Milano, Italy

[2] Lombard Museum of Agricultural History, Via Celoria, 2, 20133 Milano, Italy

[3] DiSAA, Università degli Studi di Milano, Via Celoria 2, 20133 Milano, Italy

[4] Biotechnology and Agroindustry Division, ENEA (Italian National Agency for New Technologies, Energy and Sustainable Economic Development), Casaccia Research Center, via Anguillarese 301, 00123 Rome, Italy

[5] Center for the Analysis of Sustainable Agricultural Systems (www.casasglobal.org), Kensington CA 94707, USA

[6] UO Veterinaria, DG Welfare, Regione Lombardia, P.zza Città di Lombardia 1, 20124 Milano, Italy

[7] DMMT, University of Brescia, Viale Europa 11, 25123 Brescia, Italy

[8] Department of Life Sciences, University of Modena and Reggio Emilia, Via G. Amendola 2, 42122 Reggio Emilia, Italy

Abstract

The Asian tiger mosquito (*Aedes albopictus*) is one of the most invasive disease vectors worldwide. The species is a competent vector of dengue, chikungunya, Zika viruses and other severe parasites and pathogens threatening human health. The capacity of this mosquito to colonize and establish in new areas (including temperate regions) is enhanced by its ability of producing diapausing eggs that survive relatively cold winters. The main drivers of population dynamics for this mosquito are water and air temperature and photoperiod. In this paper, we present a mechanistic model that predicts the potential distribution, abundance and activity of Asian tiger mosquito in Europe. The model includes a comprehensive description of: i) the individual life-history strategies, including diapause, ii) the influence of weather-driven individual physiological responses on population dynamics and iii) the density-dependent regulation of larval mortality rate. The model is calibrated using field data from several locations along an altitudinal gradient in the Italian Alps, which enabled accurate prediction of cold temperature effects on population abundance, including identification of conditions that prevent overwintering of the species. Model predictions are consistent with the most updated information on species' presence and absence. Predicted population abundance shows a clear south-north decreasing gradient. A similar yet less evident pattern in the activity of the species is also predicted. The model represents a valuable tool for the development of strategies aimed at the management of *Ae. albopictus* and for the implementation of effective control measures against vector-borne diseases in Europe.

Keywords: population dynamics, *Ae. albopictus*, stage-structured population, demographic model

1. Introduction

The Asian tiger mosquito, *Aedes albopictus* (Skuse, 1894) (Diptera: Culicidae), is one of the most invasive disease vectors worldwide (Benedict et al., 2007; Medlock et al., 2012; Paupy et al., 2009). In less than 40 years, this species has spread from its native distribution area (southeast Asia) to all inhabited continents (Knudsen, 1995; Kraemer et al., 2015; Moore and Mitchell, 1997). Since the first finding of *Ae. albopictus* in Europe, recorded in Albania in 1979 (Adhami, 1998), the mosquito rapidly established in southern and central Europe in the following decades (Medlock et al., 2012) reaching Germany (Kulisch et al al., 2018) and Czech Republic (Rudolf et al., 2018). The dispersal of this species across continents is due to passive transportation of eggs via the global trade of used tires or other materials in which eggs can be laid and survive (Reiter and Sprenger, 1987). Once established, the dispersal of adult individuals is facilitated by passive ground transportation (Medlock et al., 2012; Rudolf et al., 2018). The success of *Ae. albopictus* in establishing in temperate latitudes is due to the capacity of producing diapausing eggs able to survive relatively cold winters (Benedict et al., 2007; Kuhlisch et al., 2018; Reiter, 1998). The Asian tiger mosquito has been recognized as competent vector for a range of severe human pathogens and parasites among which dengue, chikungunya, Zika and occasionally west Nile viruses (Couto-Lima et al., 2017; Gratz, 2004; Guo et al., 2013; Leta et al., 2018; Paupy et al., 2009; Shragai et al., 2017; Stanaway et al., 2016) becoming responsible of a growing public health concern. The recent autochthonous outbreaks of chikungunya and dengue in the European Mediterranean area (Angelini et al., 2007; Gjenero-Margan et al., 2011; La Ruche et al., 2010; Manica et al., 2017) underlined the urgent need of developing new strategies for evaluating the risks of transmission of emerging pathogens in not autochthonous epidemiological niches. These strategies include rigorous monitoring systems and tools describing the phenology and the population dynamics of the mosquito in the current and in the potential area of distribution (Fischer et al., 2014).

Several studies have tried to define the area of potential distribution, abundance or habitat suitability of *Ae. albopictus* throughout the development of models coupled with Geographic Information Systems (GIS) considering the influence of environmental and climatic variables (for a review, see Fischer et al. (2014)). Among others, temperature, photoperiod and precipitation patterns have been identified as the most influencing drivers in determining the mosquito habitat suitability (Brady et al., 2013; Campbell et al., 2015; Sallam et al., 2017; Tran et al., 2013).

The modelling approaches used for predicting the potential distribution of *Ae. albopictus* mainly refer to correlative (statistical) and mechanistic approaches. Correlative models are based on investigating the correlation existing between one or more variables and the current occurrence of the species. The main outputs of these models refers to species habitat suitability or potential spatial distribution (Benedict et al., 2007; Ding et al., 2018; Kraemer et al., 2019; Proestos et al., 2015; Santos and Mesenes, 2017; Sanz-Aguilar et al., 2018; Trájer et al., 2014). Despite their wide use, correlative approaches might have some limitations in predicting the potential distribution of the investigated species. The lack of exhaustive presence-absence datasets and difficulties in interpreting the real area of distribution (e.g. misidentification of the species, presence of transient populations, ongoing spread in new areas etc.) might lead to wrong interpretation of the habitat suitability of the species (Kobayashi et al., 2002; Soberón and Peterson, 2011). Furthermore, these modelling approaches do not provide information on species potential abundance and impacts in the assessed area. The interpretation of habitat suitability indexes in the context of risk assessment is problematic, since the meaning of these indexes cannot be interpreted in terms of population abundance

neither in any other variable directly related to the impact of a vector. On the other hand, mechanistic models do not require full datasets of presence-absence records, since they are able to predict the population dynamics based on individual traits and physiological responses to environmental driving variables. Furthermore, these types of models allow predicting the potential species population abundance, thus providing a direct link to the impacts of that species in the assessed area (Erguler et al., 2016; Gilioli et al., 2014; Gutierrez, 1996; Gutierrez and Ponti, 2013). Projections of vector population abundance can also account for individual variability and non-linearity in the responses to environmental drivers (Soberón and Nakamura, 2009). A complete overview on the main differences between mechanistic and statistical modelling approaches applied to *Ae. albopictus* is presented in Brady et al. (2014) and Fischer et al. (2014). The first mechanistic models were based on the selection of relevant variables (mean temperature in January, annual rainfall, photoperiod etc.) used for setting up climatic constraints for predicting the areas of potential establishment and mosquito seasonal activity (ECDC, 2009; Kobayashi et al., 2002; Medlock et al., 2006). These models were used for simulating *Ae. albopictus* climate suitability and seasonal activity locally (Petrić et al., 2017) and at European level (Caminade et al., 2012).

The first stage-structured model simulating *Ae. albopictus* local population dynamics was developed by Erickson et al. (2010). Subsequent developments referred to the implementation of mechanistic models of vector dynamics coupled with a model for the disease dynamics for the assessment of vector-borne disease epidemics (Erguler et al., 2017; Erickson et al., 2012; Guzzetta et al., 2016a,b; Mordecai et al., 2017; Poletti et al., 2011). Other mechanistic models included the influence of diapause on inter-annual mosquito population dynamics (Erguler et al., 2016, 2017; Jia et al., 2016; Tran et al., 2013; Zheng et al., 2018). Some models included also the potential role of climate change on mosquito population dynamics (Gilioli et al., 2015; Jia et al., 2017) and on habitat suitability (Metelmann et al., 2019).

In this paper, we present a weather-driven, spatially-explicit, mechanistic model based on a system of partial differential equations. The model gives a comprehensive description of the individual life-history strategies, including diapause, taking into account the role of biotic interaction on mosquito population dynamics throughout the application of density-dependent mortality of larvae.

The estimation of parameters referring to larval density-dependent mortality is performed using average egg counts obtained by ovitrap captures in seven locations of the Bolzano Province (Italy) following an altitudinal gradient. Other parameters linked to development, mortality and fecundity of *Ae. albopictus* are estimated separately by fitting functions to experimental data collected from literature.

The aim of our work is to predict: i) the area of potential establishment, ii) the potential population abundance iii) the seasonal population activity (expressed as the number of weeks between the spring egg hatching and the beginning of autumn egg diapause) of *Ae. albopictus* females in Europe. Predicted population abundance and seasonal population activity can be regarded as proxies of the species habitat suitability or alternatively, they can be used to infer the potential impact of *Ae. albopictus* in the assessed area.

The paper is organized as follows: in Section 2 we describe the demographic model for *Ae. albopictus*; in Section 3 we present the methodology followed to generate weather data, and data on eggs abundance used for model calibration; in Section 4 we present the results of the calibration procedure and the maps representing the area of potential distribution, abundance and activity of *Ae. albopictus* in Europe; in Section 5 we discuss the main results and provide concluding remarks.

2. The mathematical model

The population dynamics of *Ae. albopicuts* is represented by a system of Fokker-Planck partial differential equations, already presented in Buffoni and Pasquali (2007). It is a stage-structured demographic model that has been applied to other species in Gilioli et al. (2014, 2016, 2017a,b,c), and Lanzarone et al. (2017), and also in Pasquali et al. (2019) in its simplified form of phenological model.

Assume the population composed by s stages. Denote by $\phi^i(t,x)$ $(i=1,2,3,4)$ the abundance of individuals in stage i $(i=1,2,...,s)$ at time t, with physiological age x, that is the percentage of development of an individual in a stage. Let $v^i(t)$ and $m^i(t)$ be the stage-specific development and mortality rates, respectively. The population dynamics is described by the system:

$$\frac{\partial \phi^i}{\partial t} + \frac{\partial}{\partial x}\left[v^i(t)\phi^i - \sigma^i\frac{\partial \phi^i}{\partial x}\right] + m^i(t)\phi^i = 0, \quad t > t_0, \ x \in (0,1), \tag{1}$$

$$\left[v^i(t)\phi^i(t,x) - \sigma^i\frac{\partial \phi^i}{\partial x}\right]_{x=0} = F^i(t), \tag{2}$$

$$\left[-\sigma^i\frac{\partial \phi^i}{\partial x}\right]_{x=1} = 0, \tag{3}$$

$$\phi^i(t_0,x) = \hat{\phi}^i(x), \tag{4}$$

where the functions $\hat{\phi}^i(x)$ $(i=1,2,...,s)$ are the initial distributions, and the σ^i are the diffusion coefficients, that allow to take into account the variability of development rate among individuals. The functions $F^i(t)$ represent the fluxes from a stage to the next one. More precisely, $F^1(t)$ is the egg production flux and it is given by:

$$F^1(t) = \int_0^1 a_0(T(t))\, f(x)\phi^s(t,x)\, dx \tag{5}$$

where $a_0(T(t))\, f(x)$ is the number of eggs produced per adult with physiological age in $(x, x+dx)$ per time unit, $a_0(T(t))$ takes into account the effect of time-dependent temperature $T(t)$ and $f(x)$ is the maximum age specific fertility profile. In our model, we include the influence of diapause. In particular, diapause depends on daylight D and on time t. Thus, equation (5) is modified as follows:

$$F^1(t) = \begin{cases} (1-diap(D))\int_0^1 a_0(T(t))\, f(x)\phi^s(t,x)\, dx & for \ t \in [t_{min}^{diap}, t_{max}^{diap}], D \leq D_{max} \\[2mm] \int_0^1 a_0(T(t))\, f(x)\phi^s(t,x)\, dx + A_{diap} & \begin{array}{c} the\ first\ t\ out\ of\ [t_{min}^{diap}, t_{max}^{diap}] \\ when\ D \geq D_{min}, \bar{T}_{min} \geq T_d \end{array} \\[2mm] \int_0^1 a_0(T(t))\, f(x)\phi^s(t,x)\, dx & otherwise \end{cases} \tag{6}$$

where $diap(D)$ is the percentage of eggs entering diapause (depending on daylight D), $\bar{T}_{min}$ is the average of the minimum temperature of the previous week, D_{max} is the maximum daylight under which the diapause is active, D_{min} is the minimum daylight over which the diapause end, t_{min}^{diap} is the initial time of diapause, t_{max}^{diap} is the final time of diapause, and A_{diap} is the number of diapausing eggs accumulated during the period in which diapause is active.

For $i > 1$, the fluxes from stage $i - 1$ to stage i are given by

$$F^i(t) = v^{i-1}(t)\phi^{i-1}(t,1), \qquad i = 2, \dots, s. \tag{7}$$

The number of individuals in stage i at time t can be obtained integrating functions $\phi^i(t,x)$ over the physiological age:

$$N^i(t) = \int_0^1 \phi^i(t,x)dx. \tag{8}$$

In this model we assume that the host's availability and the availability of breeding sites are not limiting factors, then they do not affect the basic demographic processes (development, mortality, fecundity).

2.1. Biodemographic functions for Ae. albopictus

We assume the population of *Ae. albopictus* being composed by five stages: four immature stages (eggs, larvae, pupae, sexually immature adults), and an adult reproductive stage. For each stage, development and mortality rate functions are specified. Moreover, for the reproductive adult stage also the fecundity rate function is stated. Fitted functions and literature data for biodemographic rate functions are reported in the Supplementary Materials.

2.1.1. Development rate function
Development times of *Ae. albopictus* are available in literature for eggs, larvae, pupae, and sexually immature adults: for the egg stage, data come from Delatte et al. (2009) and from Monteiro et al. (2007); for the larval and the pupal stages, data come from Delatte et al. (2009), Hien (1975), and Monteiro et al. (2007); for the sexually immature adults, data come from Calado and Navarro-Silva (2002), and Delatte et al. (2009).

For each developmental stage, we choose a function that well represent literature data. Egg development rate, is described by a third degree polynomial (see Kontodimas et al., 2004):

$$v^1(T(t)) = \begin{cases} aT^2(T_{sup} - T) & 0 \le T \le T_{sup} \\ 0 & otherwise \end{cases} \tag{9}$$

while, for the development rates of larvae, pupae and sexually immature adults we use the Brière function (Brière et al., 1999):

$$v^i(T(t)) = \begin{cases} aT(T - T_{inf})\sqrt{T_{sup} - T} & T_{inf} \le T \le T_{sup} \\ 0 & otherwise \end{cases} \qquad i = 2,3,4 \,. \tag{10}$$

The parameters a, T_{inf}, and T_{sup} in equations (9) and (10) are estimated using a least square estimation method (Table 1).

Table 1. Estimates of parameters in equations (9) and (10) for the pre-reproductive stages.

	a	T_{inf} (ºC)	T_{sup} (ºC)
Eggs	0.0000416657		37.3253
Larvae	0.00008604	8.2934	36.0729
Pupae	0.0003102	11.9433	40
Sexually immature adults	0.0001812	7.7804	35.2937

Data on the life-span of reproductive adults are not available in literature. Thus, the reproductive adult development rate function is obtained in a different way that involves the definition of the fecundity rate function (see the Subsection 2.1.3).

2.1.2. Mortality rate function

The mortality rate function is obtained from the average stage proportional mortality as function of temperature. Data on the proportion of dying individuals can be found in literature for eggs, larvae, and pupae. For these stages, the proportion of dying individuals can be described by a second order polynomial:

$$M^i(T(t)) = \begin{cases} p_1 T^2 + p_2 T + p_3 & T_{inf} \leq T \leq T_{sup} \\ p_1 T_{inf}^2 + p_2 T_{inf} + p_3 & T < T_{inf} \\ p_1 T_{sup}^2 + p_2 T_{sup} + p_3 & T > T_{sup} \end{cases} \qquad i = 1,2,3 \qquad (11)$$

where T_{inf} and T_{sup} are the minimum and maximum temperatures so that $M^i(T)$ assumes a maximum value of 0.9.

Then, the mortality rate function is defined as follows (see Gilioli et al., 2016):

$$\mu^i(T(t)) = \begin{cases} -v^i(T(t))\log\left(1 - M^i(T(t))\right) & T_{inf}^\mu \leq T \leq T_{sup}^\mu \\ -v^i(T_{inf})\log\left(1 - M^i(T_{inf})\right)\left[a\left(T_{inf} - T\right)^2 + 1\right] & T < T_{inf}^\mu \\ -v^i(T_{sup})\log\left(1 - M^i(T_{sup})\right)\left[b\left(T - T_{sup}\right) + 1\right] & T > T_{sup}^\mu \end{cases} \qquad i = 1,2,3 \qquad (12)$$

with the interval $\left[T_{inf}^\mu, T_{sup}^\mu\right]$ contained in the interval of positivity of the development rate function. Parameters in function (11) are obtained by fitting literature data in Delatte et al. (2009) throughout a least square method (Table 2).

Table 2. Parameters of the average stage proportional mortality (11) for eggs, larvae, and pupae.

	p_1	p_2	p_3	T_{inf} (ºC)	T_{sup} (ºC)
Eggs	0.002869	-0.1417	2.1673	11.72	37.69
Larvae	0.002793	-0.1255	1.5768	6.27	38.65

Pupae	0.003289	-0.1437	1.6197	5.77	37.93

Parameters a and b in function (12) are chosen to obtain the desired slope for low and high temperatures assuring a well connection with the shape of the function μ^i in the interval $\left[T_{inf}^{\mu}, T_{sup}^{\mu}\right]$ (granting in the two points T_{inf}^{μ} and T_{sup}^{μ} only the continuity of the function μ^i). Values of parameters a, b, T_{inf}^{μ}, T_{sup}^{μ} are reported in Table 3.

Table 3. Parameters of the mortality rate functions (12).

	a	b	T_{inf}^{μ} (ºC)	T_{sup}^{μ} (ºC)
Eggs	0.05	0.018	12	30.5
Larvae	0.2	0.15	17	30.5
Pupae	0.1	0.2	17	37.5

Data on the proportion of dying adults are not available separately for sexually immature and reproductive adults. Then the choice is to consider, for these two stages, the same mortality function that is assumed a constant parameter to be estimated (see the Subsection 2.1.3).
We assume a density-dependent larval mortality described by the function:

$$m^2\big(T(t)\big) = \mu^2\big(T(t)\big)\big(1 + \alpha N^2(t)\big)^{\beta} \tag{13}$$

obtained using a simple power function, where $N^2(t)$ is the number of larvae (stage 2) present in the system at time t, while α and β are two constant parameters to be estimated. The power function proposed for the density-dependence in the mortality rate is more flexible than the linear function used in Guzzetta et al. (2016b), and in Jia et al. (2016). For the other stages, we do not assume density-dependent mortality.

$$m^i(T) = \mu^i(T) \qquad i = 1,3,4,5.$$

2.1.3. *Fecundity rate function and the reproductive adult stage*
The fecundity function is assumed to be influenced only by temperature, that is reproductive females produce the same number of eggs independently of the physiological age. We choose a Brière function to describe the temperature-dependent fecundity rate of reproductive adults:

$$a_0(T(t))f(x) = \begin{cases} aT\big(T - T_{inf}\big)\sqrt{T_{sup} - T} & T_{inf} \leq T \leq T_{sup} , \quad 0 \leq x \leq 1 \\ 0 & otherwise \end{cases} \tag{14}$$

Development, mortality and reproduction for adults are modeled together using data on fecundity and longevity reported by Delatte et al. (2009). Data on the duration of the oviposition period (Delatte et al. 2009), calculated for a survival of 1% (Table 4), allow to obtain the reproductive adult development rate which is approximately constant and equal to 0.015 *1/day*. Parameters of the fecundity rate function (14) are estimated (Table 5) using a nonlinear regression method to fit the total number of eggs laid by a female (Table 4, second row) at fixed temperatures. The simulated number of eggs laid by a female is obtained integrating (14) on the physiological age using the parameters in Table 5 and the constant development rate of 0.015 *1/day*. Results are reported in Table 4 (third row).

Table 4. First row: oviposition period considering a survival of 1%; second row: total number of eggs/female (Delatte et al., 2009); third row: simulated total number of eggs/female of *Ae. albopictus* at different temperatures.

	T=15 ºC	T=20 ºC	T=25 ºC	T=30 ºC	T=35 ºC
Oviposition period	65	63.11	64.46	75.83	30.17
Total number of eggs/female (Delatte et al., 2009)		60.39	150.8	195.04	20.2
Total number of eggs/female (simulated)		62.03	147.59	196.93	20.17

Table 5. Parameters of the fecundity rate functions (14) of *Ae. albopictus* obtained using a nonlinear regression method on the total number of eggs laid by a female. In parenthesis the SD of the estimates.

a	T_{inf} (ºC)	T_{sup} (ºC)
0.0032	16.24	35.02
(0.00012)	(0.3454)	(0.0085)

Given the selected development and fecundity rate functions, the mortality rate for the adults are estimated to well approximate the net reproductive rate reported by Delatte et al. (2009) using a least square method (Table 6). The value obtained for the adult mortality rate is 0.067 *1/day*, and it is used also as mortality rate for the sexually immature adult stage.

Table 6. Net reproductive rates of *Ae. albopictus* (Delatte et al., 2009) and simulated net reproductive rate (using an adult mortality of 0.067) at different temperatures.

	T=20 ºC	T=25 ºC	T=30 ºC	T=35 ºC
Net reproductive rate (Delatte et al., 2009)	11.05	33.08	43.29	0.04
Net reproductive rate (simulated)	13.56	32.26	43.05	4.32

2.2. Diapause

In our model, a certain percentage of mosquito eggs enters in diapause and survive to winter temperatures. We assume this percentage depending on the daylight period, following the formula:

$$diap(D) = \frac{1}{1 + e^{3.04(D-12.62)}}$$

where D represents the daylight period in hours (Lacour et al., 2015).

To model diapause, a storage of eggs A_{diap} has been created starting from $t_{min}^{diap} = 1^{st}$ July up to $t_{max}^{diap} = 31^{st}$ December, when daylight is less than or equal to $D_{max} = 15$ hours. Diapausing eggs are subject to mortality. Fitting data on the surviving eggs after diapause reported in Thomas et al. (2012) we obtain the following diapausing egg mortality rate:

$$m^{diap}(T) = 0.05301e^{-0.1649T}.$$

As soon as the daylight is equal or greater than $D_{min} = 11.25$ hours and the average of the minimum temperature of the previous week is equal or greater than $T_d = 12.5$ °C the survived eggs stored in A_{diap} break the diapause state. Then, the eggs start again the development from physiological age 0 following the rate function (9).

3. Data

To run the model, data on temperature and daylight duration are needed. Biodemographic functions of adults are regulated by air temperature, while biodemographic functions of immature stages are driven by 5 cm depth water temperature.

Data on presence of mosquito eggs are available for some locations in Bolzano province. Hourly temperature data for these locations were simulated on the basis of daily time series of maximum and minimum air temperature (Tx, Tn) from nine weather stations located in Vipiteno, Bressanone, Brunico, Bolzano and Salorno (Meteorological Service of the Autonomous Province of Bolzano), Rovereto, Mori-Loppio, San Michele all'Adige and Aldeno (Meteotrentino). To generate hourly temperature data, we apply the following algorithm:

1. For the observation sites the daily Tx, Tn for the average year (mean of the period 2000-2012) are rebuild on the basis of Tx and Tn of the nine weather stations. To do it, a suitable geo-statistical procedure consisting of weighted averages, with weight inversely proportional to squared distances is applied to the data of the weather stations previously homogenized to the observation point for height and aspect by the method described in section S1 of the Supplementary materials. The adopted weighting procedure makes negligible the contribution of more remote stations;

2. Tx and Tn for each reference point are then adopted to simulate hourly air temperatures by means of the de Wit's algorithm (de Wit et al., 1978);

3. A reference year with 8760 hourly values are obtained by averaging hourly values of the original period 2000-2012;

4. Hourly water temperatures at 5 cm of depth for the reference year are then obtained by means of a semi-empirical model based on the Fourier equation of heat diffusion (Larnier et al., 2010) applied to hourly air temperatures (see Supplementary material section S2).

Data on egg population dynamics were made available by the Agency for the Environment and Climate Protection of the Bolzano Province (Italy), and used to calibrate the parameters of the density-dependent larval mortality rate of *Ae. albopictus*. These data refer to the weekly mean abundance of eggs collected from ovitraps deployed in seven locations (Brunico, Vipiteno, Appiano, Caldaro, Bressanone, Bolzano and Laives) of the Bolzano Province in the reference period 2013-2015. A total number of 105 georeferenced ovitraps were monitored in the area (6 in Brunico, 6 in Vipiteno, 9 in Appiano, 8 in Caldaro, 8 in Bressanone, 53 in Bolzano and 15 in Laives). The egg population abundance in each site is expressed as the mean number of eggs sampled per week in the reference period. Egg abundance is calculated considering only samples with number of eggs greater than zero. Where samples are always zero, egg abundance is set equal to zero and the site is considered outside the area of potential distribution. We purposely chose sites in a wide altitudinal range to test model's capability to predict the presence, the absence and eventually the abundance of mosquito eggs under varying meteorological regimes (Table 7). Since 2013, treatment and monitoring campaigns aimed at preventing the spread of *Ae. albopictus* have

started in the Bolzano Province. Having not clear indications and data aimed at quantifying the potential role of treatments on the overall mosquito population distribution and abundance in the reference area it was not possible to include this aspect in the model. Therefore, we introduce the simplifying assumption that the effect of treatments on the overall mosquito population distribution and abundance was negligible.

Table 7. Geographic coordinates of the centroid of the area in which eggs are sampled, in the seven locations of the Bolzano Province. For each centroid is reported the altitude in *m* a.s.l..

Location	Latitude (°N)	Longitude (°E)	Altitude (*m*)	Mosquito Presence/absence
Brunico	46°47'16,29"	11°56'17,06"	830	Absent
Vipiteno	46°53'33,01"	11°26'00,66"	949	
Appiano	46°27'34,38"	11°15'00,46"	516	Present (population density ≤ 30 eggs/week)
Caldaro	46°24'31,77"	11°13'58,24"	530	
Bressanone	46°44'03,58"	11°38'29,23"	626	
Bolzano	46°30'26"	11°21'11"	290	Present (population density > 30 eggs/week)
Laives	46°26'15"	11°20'49"	250	

To obtain an estimate of α and β in (13), data on egg abundance in the different locations of the Bolzano province are used (Table 8). A procedure similar to that used for the sites of the Bolzano Province was also applied in order to rebuild meteorological data for the whole European area (grid with pixel 0.25×0.25 degrees lat - lon referred to a rectangular area ranging from 34° to 72° North and -11° to 42° East). In such case the daily time series 2000-2012 of Tx, Tn for each cell are produced by a suitable interpolation procedure (weighted average with weight inversely proportional to squared distances on data previously homogenized for the height adopting a lapse rate of -0.5°C/100 m) applied to maximum and minimum temperatures from synoptic meteorological stations beginning to the NOAA-GSOD dataset (National Oceanic and Atmospheric Administration, National Climatic Data Centre, Global Summary Of the Day). Also in this case hourly air temperatures (AT) are obtained by means of the de Wit algorithm (de Wit et al., 1978) and hourly water temperatures are obtained by means of a semi-empirical model based on the Fourier equation of heat diffusion (Larnier et al., 2010).

4. Results

4.1. Model calibration

The model is calibrated estimating the parameters of a density-dependent mortality rate function for the *Ae. albopictus* larvae. To run the model an initial population of 100 adults at 1st of May, with physiological age uniformly distributed between 0 and 1, is considered. Air temperature is used for simulating the population abundance of the adult stage while water temperature at 5 cm depth is used for simulating the population

dynamics of the immature stages. A reference year of 8760 hourly values is obtained averaging hourly values of the original period 2000-2012 as explained above.

Parameters α and β in formula (13) are estimated using a least square method in order to minimize the difference between the simulated and the mean number of observed eggs per week in the different locations of the Bolzano province. In particular, we solve the problem:

$$\min_{\alpha,\beta} \sum_{i=1}^{7} \left(\bar{N}_i^1(\alpha,\beta) - E_i\right)^2$$

where $\bar{N}_i^1(\alpha,\beta)$ is the mean number of eggs simulated in the location i, depending on the parameters α,β, while E_i is the number of eggs collected in the same location.

The mean number of eggs in the simulation is obtained running the model for 20 years in order to obtain a stable pattern of population dynamics and the yearly mean over the last year is used. In table 8 are reported the results of model calibration. The model is able to predict the mean number of eggs in the locations where the species is present. Where the mosquito is not established (Brunico and Vipiteno) the model correctly predicted the absence of eggs. The values of the estimated parameters are $\alpha = 0.1606$, $\beta = 0.5133$, with 95% confidence intervals $[0.0145, 1.7787]$ and $[0.1179, 0.9087]$, respectively.

Table 8. Mean number of mosquito eggs in the different locations of the Bolzano Province. Only locations in which the mosquito is present are here considered.

Location	Mean number of observed eggs/week	Estimated number of eggs
Appiano	13.96	26.77
Caldaro	21.38	18.20
Bressanone	2.05	5.08
Bolzano	80.77	72.07
Laives	112.63	115.46

4.2. Maps of mosquito potential distribution, abundance and activity

The calibrated model is used for deriving maps representing the area of potential distribution, abundance and activity (expressed as number of weeks between the spring egg hatching and the beginning of autumn egg diapause) of *Ae. albopictus* in each location of a 0.25 x 0.25° lat lon grid covering Europe. We run the model for each point of the grid, using 100 adults at 1st of May, with physiological age uniformly distributed between 0 and 1 as initial conditions. In each point, the simulation covers a 10 years period. An index of mosquito population abundance is derived by calculating the mean number of adult females per area unit over the last year of simulation. This index is mapped for the simulated area in Fig. 1.

The model predicts an area of potential distribution that comprises the Iberian peninsula, most of France and Italy, the Balkan peninsula and large parts of Hungary, Romania and Ukraine. Isolated populations might be present in some areas of central Europe where climate is more favourable. The model predicts the

presence of *Ae. albopictus* in central Germany and in southern Czech Republic in agreement to the latest detections reported in Kuhlisch et al. (2018) and Rudolf et al. (2018), respectively. The predicted population abundance shows a negative gradient from southern to northern Europe. The highest population abundance is predicted for the Mediterranean countries particularly in proximity of the coastal areas (especially in the Italian peninsula, southern Spain, southern Portugal and southern France).
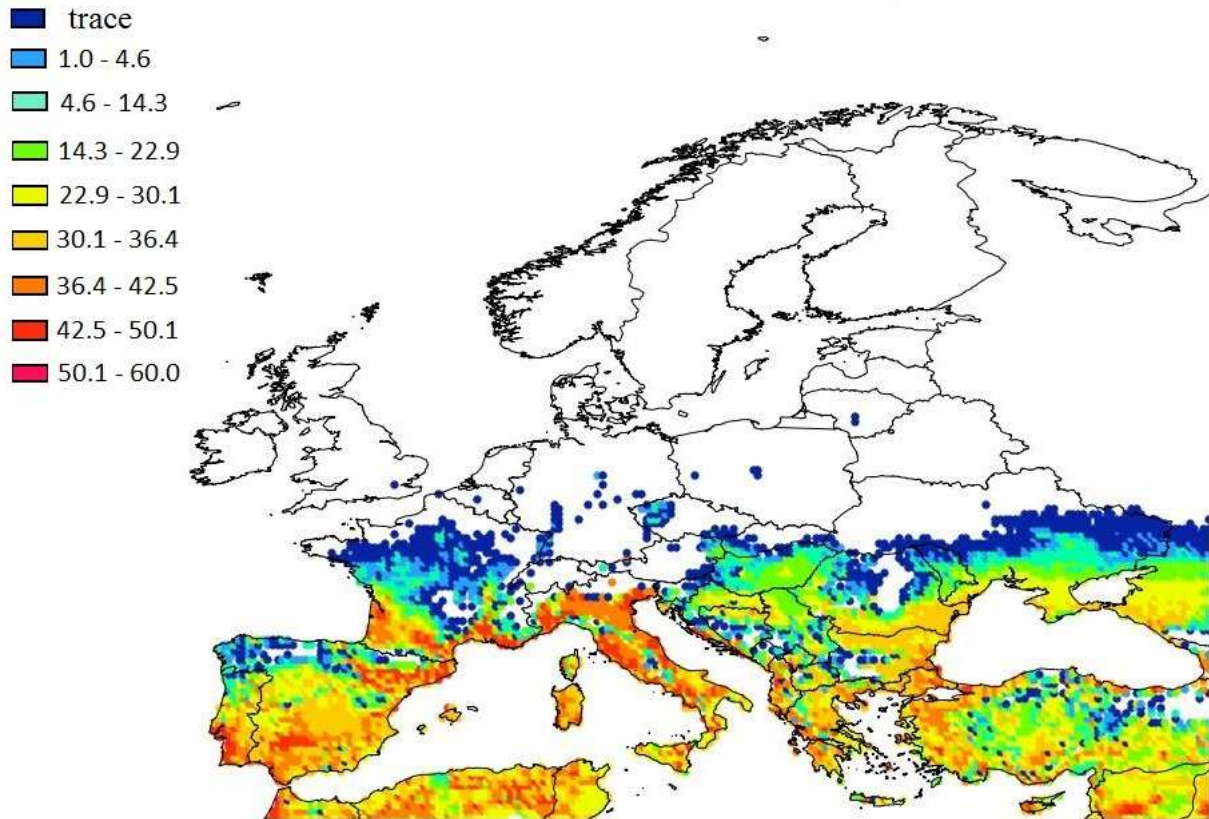
Figure 1. Heat map showing the simulated index of *Ae. albopictus* population abundance (mean number of adult females per area unit on the last year of simulation) in Europe. Temperature data used in the model refer to the period 2000-2012. The dark blue colour class is defined as 'trace' and represents areas in which the abundance is positive and less than 1.

Another important aspect linked to the potential impact of a vector is represented by the seasonal activity period, i.e. the time between egg hatch and the beginning of diapause (Caminade et al., 2012; ECDC, 2009; Medlock et al., 2006). The outputs of the simulation are shown in Fig. 2. The highest population activity (up to 19 weeks) is found in southern Europe (especially in the south of Spain, Portugal, Greece, Italy, Cyprus, and Crete) mainly in the coastal areas. The seasonal activity decreases towards the northern distribution limit of the species with a less evident gradient respect to population abundance.
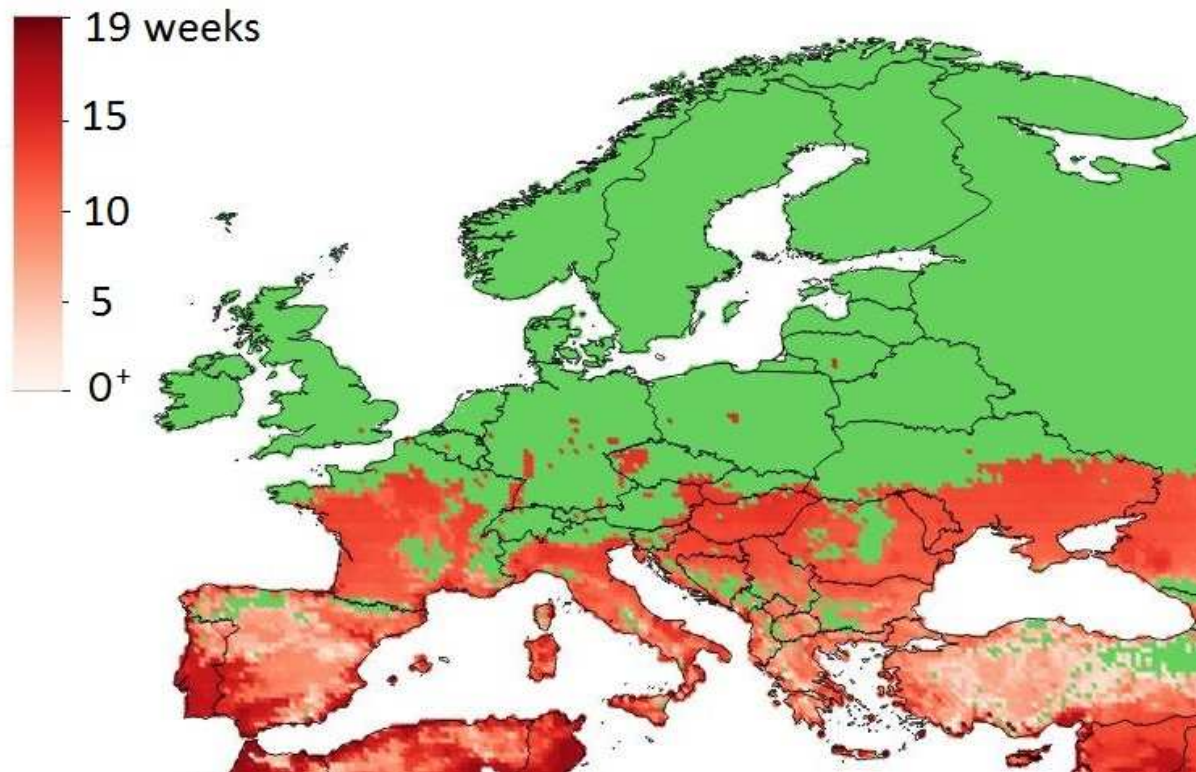
Figure 2. Simulated mosquito seasonal activity expressed as number of weeks between the spring egg hatching and the beginning of autumn egg diapause (pale pink to dark red colour gradient). The green colour refers to areas characterized by the absence of the species.

5. Discussions and conclusions

Since the first introduction in Europe, *Ae. albopictus* showed a rapid expansion of its area of establishment raising concerns related to potential vector-borne diseases outbreaks in Europe. Among other variables, temperature and precipitation patterns are major drivers in determining the habitat suitability of *Ae. albopictus*, while the duration of daylight is fundamental in triggering diapause and thus ensuring the survival towards the northern distribution limit. This work presents the results of a mechanistic model predicting the potential distribution of the species and evaluating the abundance and the seasonal period of activity as main factors in determining the impact of *Ae. albopictus* in Europe. The model aims at realistically represent the physiological and ecological responses of the species to its major abiotic drivers, specifically air temperature for adult stages, water temperature for immature stages, and both water temperature and duration of daylight for simulating diapause. Furthermore, we introduce a biotic controlling factor in terms of density-dependent mortality affecting larvae.

Overall, the simulated area of potential distribution and the northern limit comply with the most updated distribution reports of *Ae. albopictus* in Europe (ECDC and EFSA, 2019). The model is able to foresee the presence of the species in southern Europe where the favorable climate allowed its establishment. The interpretation of data related to the absence of the species must be carefully evaluated, since the mosquito

has not reached the maximum potential distribution in Europe as clearly demonstrated by the absence in south-east part of the Iberian peninsula as well as many other parts of the Mediterranean basin characterized by a suitable climate. Although the species has not reached a stable distribution in central Europe, the current presence of the species in southern UK, Belgium, Germany, Switzerland, Austria, Czech Republic, Romania, Serbia, Bulgaria, Hungary and Slovakia (ECDC and EFSA, 2019) is correctly predicted by the model. Furthermore, the model predicts the presence of established populations in limited areas of Poland, Lithuania, Ukraine, Moldavia and Cyprus, thus these areas might be considered as potentially suitable for the introduction of the species. Unlike ECDC and EFSA (2019), the model does not predict the presence of mosquito populations in the Netherlands. However, the mosquito populations in this country are not classified as established. Unlike some correlative models (Caminade et al., 2012; Proestos et al., 2015) the simulated potential mosquito distribution does not reach northern Europe (e.g. the south and the west part of the UK, Ireland, western Scotland and Denmark). In our model, the simulation of the diapause process makes year-round survivorship of the species (i.e. establishment) relatively independent of the mild climatic conditions found in coastal areas. This enables exploring the full potential geographic distribution of the species, including areas that may be suitable but where correlative modeling approaches may predict absence due to partial niche characterization in the underlying occurrence data (see Soberón and Nakamura, 2009).

A major output of our model is the quantification of the projected mosquito population abundance in Europe. Our model shows a sharp latitudinal gradient in respect to *Ae. albopictus* population abundance. Correlative models do not provide any information about population abundance and habitat suitability may not be considered as a proxy of potential species abundance. However, the patterns of habitat suitability projected by most correlative models show a positive east-west gradient with a clear Atlantic influence (i.e., the habitat suitability is positively influenced by the proximity of the Atlantic ocean as noticed in Portugal) (Benedict et al., 2007; Caminade et al., 2012; Fischer et al., 2014; Proestos et al., 2015). Erguler et al. (2016) provided a mosquito habitat suitability index based on the ratio between the predicted population size in a certain location and the minimum population size allowing the establishment of *Ae. albopictus*. In accordance to our model, high population abundance is expected in southern and western Spain and Portugal, southern France, the coastal areas of Italy and the coastal areas of Bulgaria and Romania. In contrast to Erguler et al. (2016) our model projections do not allow the establishment of *Ae. albopictus* above the 50th North parallel. Especially, in accordance with the most updated *Ae. albopictus* distribution maps (ECDC, 2019), our model does not allow the establishment of populations in the UK (with the exception of a single point in southern London) and in Ireland.

Another important factor in the determining the risks linked to vector-borne diseases is the mosquito seasonal activity period (Caminade et al., 2012; ECDC, 2009; Medlock et al., 2006). In our model, the activity pattern shows a less evident south-north latitudinal gradient if compared with the predicted abundance. This might be caused by the influence of the daylight length (higher in northern Europe if compared to southern Europe) which prevents a fast decrease of the activity period along the south-north latitudinal gradient.

The pattern of activity predicted in our model differs from the pattern presented in ECDC (2009) and in Caminade et al. (2012) where the east-west gradient is still prominent as well as a Mediterranean influence (i.e. the positive influence on population activity in proximity of the Mediterranean Sea).

Our model does not take into account the potential role of rainfall on physiological and ecological responses of the investigated species. However, given the fact that *Ae. albopictus* is able to produce eggs in any type of natural and/or human-made water body, this shortcoming does not have strong impact on the mosquito pattern of establishment at the large-scale. However, population abundance might be influenced by the land use, in particular in relation to the availability of water at local and meso-scale.

The reliability of any quantitative risk projection is related to the possibility of calibrating and validating model outputs, particularly if data are collected in the area where the risk is assessed. Our model is calibrated in the capacity to foresee the establishment along an altitudinal gradient up to an altitude that prevents population survival in winter. Model calibration also allows to produce realistic projections of population abundance in terms of number of eggs per area unit, considering both the influence of climate and density-dependent regulation. Calibrating the model using the eggs is of paramount importance, since the sampling of this stage produces the most reliable estimation of population abundance. The model presented in this paper might be a suitable tool for the development of knowledge-based strategies aimed at the management of *Ae. albopictus* and for the implementation of effective control measures against vector-borne diseases. The projection of seasonal activity period and mosquito population abundance might be used in combination with epidemiological models in order to produce risk maps of vector-borne diseases outbreaks in Europe at different levels of resolution (from local to continental level). At continental level, the model might support the identification of suitable areas in Europe where *Ae. albopictus* has not yet been found in order to prevent the introduction in new areas. The maps on potential distribution together with maps on expected population abundance can be used to develop surveillance programs targeting vector populations or prioritize area for vector control that are at higher risk of vector-borne diseases outbreaks. The model might be used to support the design and the implementation of precision target control activities against *Ae. albopictus*. This requires the integration of the simulation model within a decision support tool in which GIS technology allows the management of environmental information strata and model outputs at high resolution (Rossi et al., submitted). Normally these systems are suited for supporting pest control activities at limited spatial extensions with high spatial and temporal resolution data on water and air temperature, relative humidity, cloudiness, breeding sites presence, size and distribution etc. At micro-scale it is also possible to describe the effects of environmental alteration due to human activities (e.g. effect of thermal pollution due to industrial effluents, change in the land use) on mosquito population abundance.The model could also aid in assessing those mosquito control strategies based on the induction of sterility such as the conventional SIT or by the exploitation of the endosymbiont bacterium Wolbachia that can induce both sterility (Bourtzis et al., 2104; Calvitti et al., 2012; Moretti et al., 2018a; see e.g., Gutierrez et al., 2019 for how the impact of sterility could be assessed) and virus protection (Moretti et al., 2018b).

Future model developments will focus on the introduction of scenarios related to the effects of: i) control measures, ii) water availability and iii) climate change, on the overall mosquito population distribution, activity and abundance.

References

Adhami, J., & Reiter, P. (1998). Introduction and establishment of *Aedes* (Stegomyia) *albopictus* skuse (Diptera: Culicidae) in Albania. *Journal of the American Mosquito Control Association*, *14*(3), 340-343.

Angelini, R., Finarelli, A., Angelini, P., Po, C., Petropulacos, K., Macini, P., Fiorentini, C., Fortuna, C., Venturi, G., Romi, R., Majori, G., Nicoletti, L., Rezza, G., & Cassone, A. (2007). An outbreak of chikungunya fever in the province of Ravenna, Italy. *Weekly releases (1997–2007)*, *12*(36), 3260.

Benedict, M. Q., Levine, R. S., Hawley, W. A., & Lounibos, L. P. (2007). Spread of the tiger: global risk of invasion by the mosquito *Aedes albopictus*. *Vector-borne and zoonotic Diseases*, *7*(1), 76-85.

Bourtzis, K., Dobson, S. L., Xi, Z., Rasgon, J. L., Calvitti, M., Moreira, L. A., Bossin, H. C., Moretti, R., Baton, L. A., Hughes, G.L., Mavingui, P., & Gilles, J. R. L. (2014). Harnessing mosquito–*Wolbachia* symbiosis for vector and disease control. *Acta tropica*, *132*, S150-S163.

Brady, O. J., Johansson, M. A., Guerra, C. A., Bhatt, S., Golding, N., Pigott, D. M., Delatte, H., Grech, M. G., Leisnham, P. T., Maciel-de-Freitas, R., Styer, L. M., Smith, D. L., Scott, T. W., Gething, P. W., & Hay, S. I. (2013). Modelling adult *Aedes aegypti* and *Aedes albopictus* survival at different temperatures in laboratory and field settings. *Parasites & vectors*, *6*(1), 351.

Brady, O. J., Golding, N., Pigott, D. M., Kraemer, M. U. G., Messina, J. P., Reiner Jr, R. C., Scott, T. W., Smith, D. L., Gething, P. W., & Hay, S. I. (2014). Global temperature constraints on *Aedes aegypti* and *Ae. albopictus* persistence and competence for dengue virus transmission. *Parasites & vectors*, *7*(1), 338.

Brière, J. F., Pracros, P., Le Roux, A. Y., & Pierre, J. S. (1999). A novel rate model of temperature-dependent development for arthropods. *Environmental Entomology*, *28*(1), 22-29.

Buffoni, G., & Pasquali, S. (2007). Structured population dynamics: continuous size and discontinuous stage structures. *Journal of mathematical biology*, *54*(4), 555-595.

Calado, D. C., & Navarro-Silva, M. A. (2002). Influência da temperatura sobre a longevidade, fecundidade e atividade hematofágica de *Aedes* (Stegomyia) *albopictus* Skuse, 1894 (Diptera, Culicidae) sob condições de laboratório. *Revista Brasileira de Entomologia*, *46*(1), 93-98.

Calvitti, M., Moretti, R., Skidmore, A. R., & Dobson, S. L. (2012). *Wolbachia* strain w Pip yields a pattern of cytoplasmic incompatibility enhancing a *Wolbachia*-based suppression strategy against the disease vector *Aedes albopictus*. *Parasites & vectors*, *5*(1), 254.

Caminade, C., Medlock, J. M., Ducheyne, E., McIntyre, K. M., Leach, S., Baylis, M., & Morse, A. P. (2012). Suitability of European climate for the Asian tiger mosquito *Aedes albopictus*: recent trends and future scenarios. *Journal of the Royal Society Interface*, *9*(75), 2708-2717.

Campbell, L. P., Luther, C., Moo-Llanes, D., Ramsey, J. M., Danis-Lozano, R., & Peterson, A. T. (2015). Climate change influences on global distributions of dengue and chikungunya virus vectors. *Philosophical Transactions of the Royal Society B: Biological Sciences*, *370*(1665), 20140135.

Couto-Lima, D., Madec, Y., Bersot, M. I., Campos, S. S., de Albuquerque Motta, M., dos Santos, F. B., Vazeille, M., da Costa Vasconcelos, P. F., Lourenço-de-Oliveira, R., & Failloux, A.-B. (2017). Potential risk of re-emergence of urban transmission of Yellow Fever virus in Brazil facilitated by competent *Aedes* populations. *Scientific reports*, *7*(1), 4848.

Delatte, H., Gimonneau, G., Triboire, A., & Fontenille, D. (2009). Influence of temperature on immature development, survival, longevity, fecundity, and gonotrophic cycles of *Aedes albopictus*, vector of chikungunya and dengue in the Indian Ocean. *Journal of medical entomology*, *46*(1), 33-41.

de Wit, C. T., Goudriaan, J., van Laar, H. H., Penning de Vries, F. W., Rabbinge R., van Keulen, H., Louwerse, W., Sibma, L., & de Jonge, C. (1978). Simulation of assimilation, respiration and transpiration of crops. *Simulation Monographs*. Pudoc, Wageningen, The Netherlands, p. 140.

Ding, F., Fu, J., Jiang, D., Hao, M., & Lin, G. (2018). Mapping the spatial distribution of *Aedes aegypti* and *Aedes albopictus*. *Acta tropica*, *178*, 155-162.

ECDC, 2009 Development of *Aedes albopictus* Risk Maps, Technical Report 0905. Available online: http://ecdc.europa.eu/en/publications/Publications/0905_TER_Development_of_Aedes_Albopictus_Risk_Maps.pdf (accessed 10 April 2019).

ECDC and EFSA, 2019. Mosquito maps. Available online: https://ecdc.europa.eu/en/disease-vectors/surveillance-and-disease-data/mosquito-maps (accessed 10 April 2019).

Erguler, K., Smith-Unna, S. E., Waldock, J., Proestos, Y., Christophides, G. K., Lelieveld, J., & Parham, P. E. (2016). Large-scale modelling of the environmentally-driven population dynamics of temperate *Aedes albopictus* (Skuse). *PLoS One*, *11*(2), e0149282.

Erguler, K., Chandra, N. L., Proestos, Y., Lelieveld, J., Christophides, G. K., & Parham, P. E. (2017). A large-scale stochastic spatiotemporal model for *Aedes albopictus*-borne chikungunya epidemiology. *PLoS one*, *12*(3), e0174293.

Erickson, R. A., Presley, S. M., Allen, L. J., Long, K. R., & Cox, S. B. (2010). A stage-structured, *Aedes albopictus* population model. *Ecological Modelling*, *221*(9), 1273-1282.

Erickson, R. A., Hayhoe, K., Presley, S. M., Allen, L. J., Long, K. R., & Cox, S. B. (2012). Potential impacts of climate change on the ecology of dengue and its mosquito vector the Asian tiger mosquito (*Aedes albopictus*). *Environmental Research Letters*, *7*, 034003 (6pp).

Fischer, D., Thomas, S. M., Neteler, M. G., Tjaden, N., & Beierkuhnlein, C. (2014). Climatic suitability of *Aedes albopictus* in Europe referring to climate change projections: comparison of mechanistic and correlative niche modelling approaches. *Eurosurveillance, 19*(6).

Gilioli, G., Pasquali, S., Parisi, S., & Winter, S. (2014). Modelling the potential distribution of *Bemisia tabaci* in Europe in light of the climate change scenario. *Pest management science*, *70*(10), 1611-1623.

Gilioli, G., Pasquali, S., Ponti, L., Calvitti, M., Moretti, R., & Gutierrez, A. P. (2015) Modelling the potential distribution and abundance of *Aedes albopictus* in Europe in light of the climate change scenario. *Conference: Impacts of Environmental Changes on Infecious Diseases*, 23-25 March 2015, Sitges, Spain.

Gilioli, G., Pasquali, S., & Marchesini, E. (2016). A modelling framework for pest population dynamics and management: An application to the grape berry moth. *Ecological modelling*, *320*, 348-357.

Gilioli, G., Pasquali, S., Martín, P. R., Carlsson, N., & Mariani, L., (2017a). A temperature-dependent physiologically based model for the invasive apple snail *Pomacea canaliculata*. *International Journal of Biometeorology, 61*(11), 1899-1911.

Gilioli, G., Schrader, G., Grégoire, J. C., MacLeod, A., Mosbach-Schulz, O., Rafoss, T., Rossi, V., Urek, G., & van der Werf, W. (2017b). The EFSA quantitative approach to pest risk assessment–methodological aspects and case studies. *EPPO Bulletin*, *47*(2), 213-219.

Gilioli, G., Schrader, G., Carlsson, N., van Donk, E., van Leeuwen, C. H. A., Martín, P. R., Pasquali, S., Vilà, M., & Vos, S. (2017c). Environmental risk assessment for invasive alien species: A case study of apple snails affecting ecosystem services in Europe. *Environmental Impact Assessment Review*, *65*, 1-11.

Gjenero-Margan, I., Aleraj, B., Krajcar, D., Lesnikar, V., Klobučar, A., Pem-Novosel, I., Kurečić-Filipović, S., Komparak, S., Martić, R., Đuričić, S., Betica-Radić, L., Okmadžić, J., Vilibić-Čavlek, T., Babić-Erceg, A., Turković, B., Avšić-Županc, T., Radić, I., Ljubić, M., Šarac, K., Benić, N., & Mlinarić-Galinović, G. (2011). Autochthonous dengue fever in Croatia, August–September 2010. *Eurosurveillance*, *16*(9), 19805.

Gratz, N. G. (2004). Critical review of the vector status of *Aedes albopictus*. *Medical and veterinary entomology*, *18*(3), 215-227.

Guo, X. X., Zhu, X. J., Li, C. X., Dong, Y. D., Zhang, Y. M., Xing, D., Xue, R. D., Qin, C. F., & Zhao, T. Y. (2013). Vector competence of *Aedes albopictus* and *Aedes aegypti* (Diptera: Culicidae) for DEN2-43 and New Guinea C virus strains of dengue 2 virus. *Acta tropica*, *128*(3), 566-570.

Gutierrez, A. P. (1996). Applied population ecology: a supply-demand approach. *John Wiley & Sons*. New York, USA.

Gutierrez, A. P., & Ponti, L. (2013). Eradication of invasive species: why the biology matters. *Environmental entomology*, *42*(3), 395-411.

Gutierrez, A. P., Ponti, L., & Arias, P. A. (2019). Deconstructing the eradication of new world screwworm in North America: retrospective analysis and climate warming effects. *Medical and veterinary entomology*.

Guzzetta, G., Poletti, P., Montarsi, F., Baldacchino, F., Capelli, G., Rizzoli, A., Rosà, R., & Merler, S. (2016a). Assessing the potential risk of Zika virus epidemics in temperate areas with established *Aedes albopictus* populations. *Eurosurveillance*, *21*(15), 30199.

Guzzetta, G., Montarsi, F., Baldacchino, F. A., Metz, M., Capelli, G., Rizzoli, A., Pugliese, A., Rosà, R., Poletti, P., & Merler, S. (2016b). Potential risk of dengue and chikungunya outbreaks in northern Italy based on a population model of *Aedes albopictus* (Diptera: Culicidae). *PLoS neglected tropical diseases*, *10*(6), e0004762.

Hien, D. S. (1975). Biology of *Aedes aegypti* (L., 1762) and *Aedes albopictus* (Skuse, 1895) (Diptera, Culicidae). III. Effect of certain environmental conditions on the development of larvae and pupae. *Acta parasitologica polonica*, 23, 553–568.

Jia, P., Lu, L., Chen, X., Chen, J., Guo, L., Yu, X., & Liu, Q. (2016). A climate-driven mechanistic population model of *Aedes albopictus* with diapause. *Parasites & vectors*, *9*(1), 175.

Jia, P., Chen, X., Chen, J., Lu, L., Liu, Q., & Tan, X. (2017). How does the dengue vector mosquito *Aedes albopictus* respond to global warming?. *Parasites & vectors*, *10*(1), 140.

Knudsen, A. B. (1995). Global distribution and continuing spread of *Aedes albopictus*. *Parassitologia*, *37*(2-3), 91-97.

Kobayashi, M., Nihei, N., & Kurihara, T. (2002). Analysis of northern distribution of *Aedes albopictus* (Diptera: Culicidae) in Japan by geographical information system. *Journal of Medical Entomology*, *39*(1), 4-11.

Kontodimas, D. C., Eliopoulos, P. A., Stathas, G. J., & Economou, L. P. (2004). Comparative temperature-dependent development of *Nephus includens* (Kirsch) and *Nephus bisignatus* (Boheman) (Coleoptera: Coccinellidae) preying on *Planococcus citri* (Risso) (Homoptera: Pseudococcidae): evaluation of a linear and various nonlinear models using specific criteria. *Environmental Entomology*, *33*(1), 1-11.

Kraemer, M. U. G., Sinka, M. E., Duda, K. A., Mylne, A. Q., Shearer, F. M., Barker, C. M., Moore, C. G., Carvalho, R. G., Coelho, G. E., Van Bortel, V., Hendrickx, G., Schaffner, F., Elyazar, I. R. F., Teng, H.-J., Brady, O. J., Messina, J. P., Pigott, D. M., Scot, T. W., Smith D. L., Wint G. R. W., Golding, N., & Hay, S. I. (2015). The global distribution of the arbovirus vectors *Aedes aegypti* and *Ae. albopictus*. *elife*, *4*, e08347.

Kraemer, M. U. G., Reiner, R. C., Brady, O. J., Messina, J. P., Gilbert, M., Pigott, D. M., Yi, D., Johnson, K., Earl, L., Marczak, L. B., Shirude, S., Weaver, N. D., Bisanzio, D., Perkins, T. A., Lai, S., Lu, X., Jones, P., Coelho, G. E., Carvalho, R. G., Van Bortel, W., Marsboom, C., Hendrickx, G., Schaffner, F., Moore, C. G., Nax, H. H., Bengtsson, L., Wetter, E., Tatem, A. J., Brownstein, J. S., Smith, D. L., Lambrechts, L., Cauchemez, S., Linard, C., Faria, N. R., Pybus, O, G., Scott, T. W., Liu, Q., Yu, H., Wint, G. R. W., Hay, S. I., & Golding, N. (2019). Past and future spread of the arbovirus vectors *Aedes aegypti* and *Aedes albopictus*. *Nature microbiology*, *4*(5), 854.

Kuhlisch, C., Kampen, H., & Walther, D. (2018). The Asian tiger mosquito *Aedes albopictus* (Diptera: Culicidae) in Central Germany: Surveillance in its northernmost distribution area. *Acta tropica*, *188*, 78-85.

Lacour, G., Chanaud, L., L'Ambert, G., & Hance, T. (2015). Seasonal synchronization of diapause phases in *Aedes albopictus* (Diptera: Culicidae). *PloS one*, *10*(12), e0145311.

Lanzarone, E., Pasquali, S., Gilioli, G., & Marchesini, E. (2017). A Bayesian estimation approach for the mortality in a stage-structured demographic model. *Journal of mathematical biology*, *75*(3), 759-779.

Larnier, K., Roux, H., Dartus, D., & Croze, O. (2010). Water temperature modeling in the Garonne River (France). *Knowledge and Management of Aquatic Ecosystems*, (398), 04.

La Ruche, G., Souarès, Y., Armengaud, A., Peloux-Petiot, F., Delaunay, P., Desprès, P., Lenglet, A., Jourdain, F., Leparc-Goffart, I., Charlet, F., Ollier, L., Mantey, K., Mollet, T., Fournier, J. P., Torrents, R., Leitmeyer, K., Hilairet, P., Zeller, H., Van Bortel, W., Dejour-Salamanca, D., Grandadam, M., & Gastellu-Etchegorry, M. (2010). First two autochthonous dengue virus infections in metropolitan France, September 2010. *Eurosurveillance*, *15*(39), 19676.

Leta, S., Beyene, T. J., De Clercq, E. M., Amenu, K., Kraemer, M. U., & Revie, C. W. (2018). Global risk mapping for major diseases transmitted by *Aedes aegypti* and *Aedes albopictus*. *International Journal of Infectious Diseases*, *67*, 25-35.

Manica, M., Guzzetta, G., Poletti, P., Filipponi, F., Solimini, A., Caputo, B., Rosà, R., & Merler, S. (2017). Transmission dynamics of the ongoing chikungunya outbreak in Central Italy: from coastal areas to the metropolitan city of Rome, summer 2017. *Eurosurveillance*, *22*(44).

Medlock, J. M., Avenell, D., Barrass, I., & Leach, S. (2006). Analysis of the potential for survival and seasonal activity of *Aedes albopictus* (Diptera: Culicidae) in the United Kingdom. *Journal of Vector Ecology*, *31*(2), 292-305.

Medlock, J. M., Hansford, K. M., Schaffner, F., Versteirt, V., Hendrickx, G., Zeller, H., & Bortel, W. V. (2012). A review of the invasive mosquitoes in Europe: ecology, public health risks, and control options. *Vector-borne and zoonotic diseases*, *12*(6), 435-447.

Metelmann, S., Caminade, C., Jones, A. E., Medlock, J. M., Baylis, M., & Morse, A. P. (2019). The UK's suitability for *Aedes albopictus* in current and future climates. *Journal of the Royal Society Interface*, *16*(152), 20180761.

Monteiro, L. C., de Souza, J. R., & de Albuquerque, C. M. (2007). Eclosion rate, development and survivorship of *Aedes albopictus* (Skuse) (Diptera: Culicidae) under different water temperatures. *Neotropical entomology*, *36*(6), 966-971.

Moore, C. G., & Mitchell, C. J. (1997). *Aedes albopictus* in the United States: ten-year presence and public health implications. *Emerging infectious diseases*, *3*(3), 329.

Mordecai, E. A., Cohen, J. M., Evans, M. V., Gudapati, P., Johnson, L. R., Lippi, C. A., Miazgowicz, K., Murdock, C. C., Rohr, J. R., Ryan, S. J., Savage, V., Shocket, M. S., Ibarra, A. S., Thomas, M. B., & Weikel, D. P. (2017). Detecting the impact of temperature on transmission of Zika, dengue, and chikungunya using mechanistic models. *PLoS neglected tropical diseases*, *11*(4), e0005568.

Moretti, R., Marzo, G. A., Lampazzi, E., & Calvitti, M. (2018a). Cytoplasmic incompatibility management to support Incompatible Insect Technique against *Aedes albopictus*. *Parasites & vectors*, *11*(2), 649.

Moretti, R., Yen, P. S., Houé, V., Lampazzi, E., Desiderio, A., Failloux, A. B., & Calvitti, M. (2018b). Combining *Wolbachia*-induced sterility and virus protection to fight *Aedes albopictus*-borne viruses. *PLoS neglected tropical diseases*, *12*(7), e0006626.

Pasquali, S., Soresina, C., & Gilioli, G. (2019). The effects of fecundity, mortality and distribution of the initial condition in phenological models. *Ecological Modelling*, in press.

Paupy, C., Delatte, H., Bagny, L., Corbel, V., & Fontenille, D. (2009). *Aedes albopictus*, an arbovirus vector: from the darkness to the light. *Microbes and Infection*, *11*(14-15), 1177-1185.

Petrić, M., Lalić, B., Ducheyne, E., Djurdjević, V., & Petrić, D. (2017). Modelling the regional impact of climate change on the suitability of the establishment of the Asian tiger mosquito (*Aedes albopictus*) in Serbia. *Climatic Change*, *142*(3-4), 361-374.

Poletti, P., Messeri, G., Ajelli, M., Vallorani, R., Rizzo, C., & Merler, S. (2011). Transmission potential of chikungunya virus and control measures: the case of Italy. *PLoS One*, *6*(5), e18860.

Proestos, Y., Christophides, G. K., Ergüler, K., Tanarhte, M., Waldock, J., & Lelieveld, J. (2015). Present and future projections of habitat suitability of the Asian tiger mosquito, a vector of viral pathogens, from global climate simulation. *Philosophical Transactions of the Royal Society B: Biological Sciences*, *370*(1665), 20130554.

Reiter, P. (1998). *Aedes albopictus* and the world trade in used tires, 1988-1995: the shape of things to come?. *Journal of the American Mosquito Control Association*, *14*(1), 83-94.

Reiter, P., & Sprenger, D. (1987). The used tire trade: a mechanism for the worldwide dispersal of container breeding mosquitoes. Journal of the American Mosquito Control Association, 3, 494–501.

Rossi, V., Sperandio, G., Caffi, T., Simonetto, A., & Gilioli, G. (submitted). Critical success factors for the adoption of Decision Tools in IPM. *Agronomy*.

Rudolf, I., Blažejová, H., Straková, P., Šebesta, O., Peško, J., Mendel, J., Šikutová, S., Hubálek, Z., Kampen, H., & Schaffner, F. (2018). The invasive Asian tiger mosquito *Aedes albopictus* (Diptera: Culicidae) in the Czech Republic: Repetitive introduction events highlight the need for extended entomological surveillance. *Acta tropica*, *185*, 239-241.

Sallam, M., Fizer, C., Pilant, A., & Whung, P. Y. (2017). Systematic review: Land cover, meteorological, and socioeconomic determinants of *Aedes* mosquito habitat for risk mapping. *International journal of environmental research and public health*, *14*(10), 1230.

Santos, J., & Meneses, B. M. (2017). An integrated approach for the assessment of the *Aedes aegypti* and *Aedes albopictus* global spatial distribution, and determination of the zones susceptible to the development of Zika virus. *Acta tropica*, *168*, 80-90.

Sanz-Aguilar, A., Rosselló, R., Bengoa, M., Ruiz-Pérez, M., González-Calleja, M., Barceló, C., Borrás, D., Paredes-Esquivel, C., Miranda, M. A., & Tavecchia, G. (2018). Water associated with residential areas and tourist resorts is the key predictor of Asian tiger mosquito presence on a Mediterranean island. *Medical and veterinary entomology*, *32*(4), 443-450.

Shragai, T., Tesla, B., Murdock, C., & Harrington, L. C. (2017). Zika and chikungunya: mosquito-borne viruses in a changing world. *Annals of the New York Academy of Sciences*, *1399*(1), 61-77.

Soberón, J., & Nakamura, M. (2009). Niches and distributional areas: concepts, methods, and assumptions. *Proceedings of the National Academy of Sciences*, *106*(Supplement 2), 19644-19650.

Soberón, J., & Peterson, A. T. (2011). Ecological niche shifts and environmental space anisotropy: a cautionary note. *Revista Mexicana de Biodiversidad*, 82, 1348-1355.

Stanaway, J. D., Shepard, D. S., Undurraga, E. A., Halasa, Y. A., Coffeng, L. E., Brady, O. J., Hay, S. I., Bedi, N., Bensenor, I. M., Castañeda-Orjuela, C. A., Chuang, T.-W., Gibney, K. B., Memish, M. A., Rafay, A., Ukwaja, K. N., Yonemoto, N., Murray, C. J. L. (2016). The global burden of dengue: an analysis from the Global Burden of Disease Study 2013. *The Lancet infectious diseases*, *16*(6), 712-723.

Thomas, S. M., Obermayr, U., Fischer, D., Kreyling, J., & Beierkuhnlein, C. (2012). Low-temperature threshold for egg survival of a post-diapause and non-diapause European aedine strain, *Aedes albopictus* (Diptera: Culicidae). *Parasites & vectors*, *5*(1), 100.

Trájer, A. J., Bede-Fazekas, Á., Bobvos, J., & Páldy, A. (2014). Seasonality and geographical occurrence of West Nile fever and distribution of Asian tiger mosquito. *Időjárás/Quarterly Journal of the Hungarian Meteorological Service*, *118*(1), 19-40.

Tran, A., L'Ambert, G., Lacour, G., Benoît, R., Demarchi, M., Cros, M., Cailly, P., Aubry-Kientz, M., Balenghein, T., & Ezanno, P. (2013). A rainfall-and temperature-driven abundance model for *Aedes albopictus* populations. *International journal of environmental research and public health*, *10*(5), 1698-1719.

Zheng, B., Yu, J., Xi, Z., & Tang, M. (2018). The annual abundance of dengue and Zika vector *Aedes albopictus* and its stubbornness to suppression. *Ecological Modelling*, *387*, 38-48.